

© The Authors, 2024.  
Content is available under Creative Commons Attribution  
License 4.0 International (CC BY 4.0)



© Авторы, 2024 г.  
Контент доступен по лицензии Creative Commons Attribution  
License 4.0 International (CC BY 4.0)

УДК 551.465

<https://doi.org/10.30730/gtr.2024.8.3.201-211>  
<https://www.elibrary.ru/lgdfiz>  
<http://journal.imgg.ru/web/full/f2024-3-3.pdf> (In Russian)

## Waves in the marine area near Cape Svobodny (south-eastern part of Sakhalin Island)\*

*Dmitry P. Kovalev<sup>@</sup>, Peter D. Kovalev, Aleksander S. Borisov, Konstantin V. Kirillov*

*<sup>@E-mail:</sup> [d.kovalev@imgg.ru](mailto:d.kovalev@imgg.ru)*

*Institute of Marine Geology and Geophysics, FEB RAS, Yuzhno-Sakhalinsk, Russia*

**Abstract.** A study of wave processes near Cape Svobodny on the south-eastern coast of the island Sakhalin using autonomous wave recorders and a weather station has been performed. Analysis of five-month data of sea level and temperature, atmospheric pressure and wind speed revealed that there are no significant peaks for wind and infragravity (IG) waves in the wave period range 2–600 s, and the wave energy is lower at the point protected by Cape Svobodny. During storms, there is an increase in the energy of IG waves. Waves detected at periods of 14.2 seconds, 3.62 minutes, and 8.85 minutes are related to swell and edge waves propagating seaward. For explanation of short waves, the Longuet-Higgins and Stewart theory was used which describes the dispersion of swell in the surf zone and the formation of free waves. Edge waves were analyzed using the Lamb model and the Bessel function of the first kind of zero order. Modelling of wave processes propagating shoreward revealed the presence of IG waves with periods of 20–110 seconds and edge waves with periods of 4.27–7.63 minutes, confirmed by the dispersion relation for Stokes waves on a sloping bottom. Sea water temperature fluctuations of more than 7 °C with periods of 3–100 minutes affect the propagation of waves with periods longer than 3 minutes, destroying the edge and leaky waves. Analysis of wind wave characteristics showed no significant wave processes, including wind waves, in the 2–20 second period range. The maximum wave height was observed during prolonged southern winds associated with a cyclone. This study is important for understanding wave processes in this area, aiding in predicting their behaviour and impact on the coastline.

**Keywords:** wind waves, edge waves, leaky waves, infragravity waves, swell, internal waves

## Волны в морской акватории вблизи мыса Свободный (юго-восточная часть о. Сахалин)\*\*

*Д. П. Ковалев<sup>@</sup>, П. Д. Ковалев, А. С. Борисов, К. В. Кириллов*

*<sup>@E-mail:</sup> [d.kovalev@imgg.ru](mailto:d.kovalev@imgg.ru)*

*Институт морской геологии и геофизики ДВО РАН, Южно-Сахалинск, Россия*

**Резюме.** Проведено исследование волновых процессов вблизи мыса Свободный на юго-восточном побережье о. Сахалин с использованием автономных регистраторов волнения и метеостанции. Анализ пятимесячных данных уровня моря и температуры, атмосферного давления и скорости ветра выявил, что в диапазоне периодов волн 2–600 с отсутствуют значительные пики для ветровых и инфрагравитационных (ИГ) волн, а энергия волн меньше в точке, защищенной мысом Свободный. Во время штормов наблюдается рост энергии ИГ-волн. Обнаружены волны с периодами 14.2 с, 3.62 мин и 8.85 мин, связанные с зыбью и излученными волнами, распространяющимися в сторону моря. Для объяснения коротких волн использована теория Лонге-Хиггинса и Стюарта, которая объясняет рассеяние зыби в зоне прилива и образование свободных волн. С использованием формулы для стоячих волн проанализированы волны Пуанкаре. Моделирование волновых процессов, распространяющихся к берегу, показало наличие ИГ-волн с периодами 20–110 с и краевых волн с периодами 4.27–7.63 мин, подтвержденных дисперсионным соотношением для волн Стокса при плоском наклонном дне. Колебания температуры морской воды с высотой более 7 °C и периодами 3–100 мин влияют

\* The translation from Russian: Ковалев Д.П., Ковалев П.Д., Борисов А.С., Кириллов К.В. Волны в морской акватории вблизи мыса Свободный (юго-восточная часть о. Сахалин). *Геосистемы переходных зон*, 2024, т. 8, № 3. [Electronic resources]. <http://journal.imgg.ru/web/full/f2024-3-3.pdf>.  
Translated by Valeriya Maksimova

\*\* Полный текст данной статьи на русском языке размещен на сайте журнала <http://journal.imgg.ru/web/full/f2024-3-3.pdf>

на распространение волн с периодами более 3 мин, разрушая краевые и излученные волны. Анализ характеристик ветрового волнения показал, что в диапазоне периодов 2–20 с отсутствуют значительные волновые процессы, включая ветровые волны. Максимальная высота волн наблюдалась при продолжительных южных ветрах, связанных с циклоном. Проведенное исследование важно для понимания волновых процессов в данной акватории, что помогает прогнозировать их поведение и влияние на береговую линию.

**Ключевые слова:** ветровые волны, краевые волны, излученные волны, инфрагравитационные волны, зыбь, внутренние волны

**For citation:** Kovalev D.P., Kovalev P.D., Borisov A.S., Kirillov K.V. Waves in the marine area near Cape Svobodny (south-eastern part of Sakhalin Island). *Geosistemy perexodnykh zon = Geosystems of Transition Zones*, 2024, vol. 8, no. 3, pp. 201–211. <https://doi.org/10.30730/gtr.2024.8.3.201-211>; <https://www.elibrary.ru/lgdflz> [The translation from Russian: Ковалев Д.П., Ковалев П.Д., Борисов А.С., Кириллов К.В. Волны в морской акватории вблизи мыса Свободный (юго-восточная часть о. Сахалин). *Геосистемы переходных зон*, 2024, т. 8, № 3. [Electronic resource]. <http://journal.imgg.ru/web/full/f2024-3-3.pdf>]

### Funding

The research was conducted as part of the government assignment of the Institute of Marine Geology and Geophysics, Far Eastern Branch of the Russian Academy of Sciences (FWWM-2024-0002).

### Финансирование

Исследования выполнены в рамках государственного задания Института морской геологии и геофизики ДВО РАН (№ FWWM-2024-0002).

## Introduction

The Laboratory of Wave Dynamics and Coastal Currents at the Institute of Marine Geology and Geophysics, Far Eastern Branch of the Russian Academy of Sciences, conducts experimental studies of wave processes in the coastal zone of the Sea of Okhotsk near Cape Svobodny, aiming to investigate waves occurring during the passage of cyclones over the observation area. While waves with periods longer than 15 seconds – such as infragravity, edge, leaky, and other waves – are usually of interest in the coastal zone, it was also decided to study shorter waves – wind waves and swell – that affect the operation of small vessels and are associated with coastal fishing in this region.

The results of studies on wind wave dynamics and swell are well documented in numerous articles and monographs (e.g., [1–3]). However, wind wave conditions near the shore are heavily influenced by the bathymetric characteristics of the seabed and the aerographic features of the coastline, making them variable in each specific marine area. The study of wave dynamics near Cape Svobodny, where two bottom wave recorders and a meteorological station were set up at the edge of the cape, provides an excellent opportunity for a more detailed investigation of these processes.

Barotropic leaky waves in the shelf zone can only exist at frequencies above the inertial frequency. Sverdrup waves generated in the open ocean are progressive waves formed under the combined influence of gravitational forces and the Earth's rotation; when they reflect from the shore, they create Poincaré waves, which exhibit a progressive nature along the shore and stationary behavior across it [4]. In describing boundary waves, the terms “Poincaré waves” and “leaky waves” are often used synonymously [5].

Infragravity and edge waves are also the focus of extensive scientific literature [6–8]. However, similar to wind waves, detailed studies of the aquatic area near Cape Svobodny have not been conducted. We studied internal waves here, and in 2021, two ARV 14K instruments were installed in the vicinity of the cape to measure variations in bottom hydrostatic pressure, which were subsequently converted to sea level, accounting for the attenuation of short waves with depth, into sea level fluctuations (wave motion). The wave measuring devices are manufactured by SKTB “EIPA” in Uglich (<https://sktbelpa.ru>). The main relative error in bottom pressure measurements is 0.06 %, with a resolution of  $\pm 0.0008$  % of the upper measurement limit. The measurement frequency for level and temperature is one second. Measurements of atmospheric pressure fluctua-

tions and wind speed were conducted using the Vantage Pro2 Weather Station.

The objective of this research was to conduct a detailed study of various types of waves, including short wind waves and swell, as well as longer infragravity and edge waves, to assess their impact on coastal processes and the operability of small vessels. The relevance of this research stems from the need to understand the specifics of wave processes in this marine area, which is crucial for predicting their behavior and impact on the coastline, as well as for supporting coastal fishing and other activities.

### Methodology and observation data

A map of the observation area – the water body of Mordvinova Bay and Cape Svobodny in the southern part of Sakhalin Island, showing the location of wave measuring devices – is presented in Figure 1. Bottom wave recorders ARV 14K (measuring pressure range 0–20 m, accuracy  $\pm 0.06\%$ ; resolution  $\pm 0.0008\%$ ) were installed on the seabed: the device with serial number 149 at a depth of approximately 14 m, and the device with number 150 at a depth of 12 m. The installation depth of the devices corresponds to a bottom slope of about 0.011. The distance between the devices is 1.69 km. Both devices recorded sea level fluctuations and temperature with a sampling rate of one second. The Vantage Pro2 Weather Station (measuring pressure range 880–1080 hPa,

accuracy  $\pm 0.5$  hPa; wind speed range 0–67 m/s, accuracy  $\pm 1$  m/s) was installed on the lighthouse at Cape Svobodny, at a height of approximately 12 m above sea level. Atmospheric pressure and wind speed were recorded with a one-hour sampling rate. This interval was chosen due to the limited memory capacity and inaccessibility of the weather station.

The experiment took place from July 9 to December 31, 2021. The observation period covered the summer and autumn seasons, characterized by prevailing southerly winds associated with the passage of cyclones, leading to significant storms.

Data processing of the time series for sea level fluctuations, including spectral and cross-spectral analyses, was performed using the Kyma software [9, 10], which was developed for visualizing and analyzing large volumes of time series data. This software was employed to calculate spectrograms of sea level fluctuations, analyze energy distribution in different period ranges, and determine the characteristics of wave processes. Spectral analysis allowed for the identification of major wave types, such as infragravity, edge, and leaky waves. A detailed analysis was performed for each wave type, including the use of theoretical models such as the Lamb model and Bessel functions, as well as the dispersion relationship for Stokes waves when analyzing edge waves. The relationship between fluctuations in seawater temperature and the propagation of waves with periods longer than

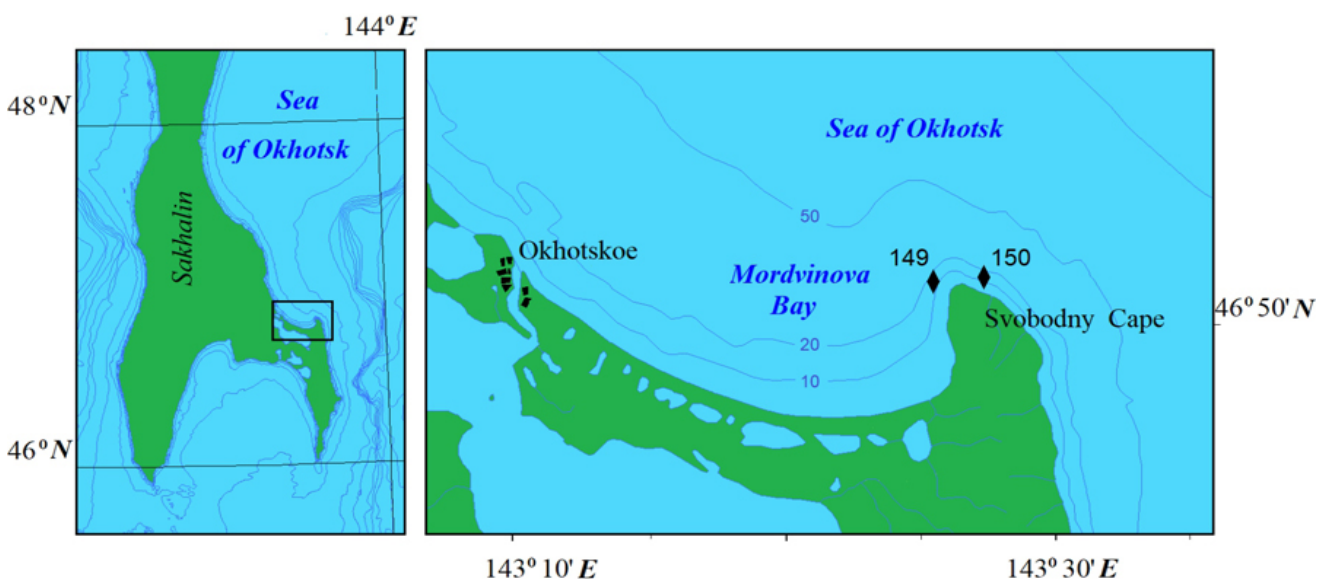


Fig. 1. The southern part of Sakhalin Island indicates the research area, including the water body of Mordvinova Bay and Cape Svobodny, with the locations of wave and temperature measuring devices.

3 minutes was also investigated, revealing the influence of internal waves on edge waves.

As a result of the observations over 5 months, records of sea level fluctuations, atmospheric pressure, and wind speed were obtained at two locations. Fragments of the records are presented in Fig 2.

The temporal series of sea level fluctuations (Fig. 2a) show tidal waves and several storms, which were more frequently observed in the autumn months – September and October. The most intense storm, with wave heights reaching 4 m, occurred in mid-September. Typically, storms, as indicated by the comparison of Fig. 2a and Fig. 2c, are accompanied by strong northerly winds.

### Analysis of sea level fluctuations

Figures 3a and 3b present spectrograms of sea level fluctuations calculated using the Kyma software [9, 10] over the range of periods for wind waves, swell, and infragravity (IG) waves. It is evident that the energy of wind waves and swell does not exhibit sharply defined maxima, and for device 149, it is somewhat lower than that of device 150. In the infragravity wave range, with periods from 20 to 250 seconds, an increase in energy is observed during storms, without a pronounced modal structure.

Since preliminary calculations indicated that the spectral density diagrams do not contain dis-

tinct features compared to those discussed in previously published works, this study focused on calculating transfer function diagrams and phases for pairs of devices. It is noteworthy that coherence functions are often used to analyze time series, which, in a linear system, indicate a causal relationship between two signals. At the same time, as indicated by statistical sampling theory, coherence estimates not only exhibit statistical variability but are also biased and significantly dependent on the number of degrees of freedom [11]. Preliminary analysis using the coherence function showed significant bias in the coherence estimates for the wave process period range discussed here. Therefore, the spectral analysis was conducted using transfer functions. As can be seen in Figures 3c and 3d, the magnitude diagrams of the transfer function proved to be quite informative.

In this article, in particular, a Bode plot, or frequency response function, is calculated, but we will use the more general term – transfer function. As shown in articles [12, 13], the transfer function is generally applied to describe the relationships between two series when one series influences another. In such cases, the gain function, or transfer function from the cross-spectrum, is typically computed using the coherence function [14]. According to the proposed research, the transfer function  $H(j\omega) = G(\omega)\phi(\omega) = |H(j\omega)| \arg(H(j\omega))$

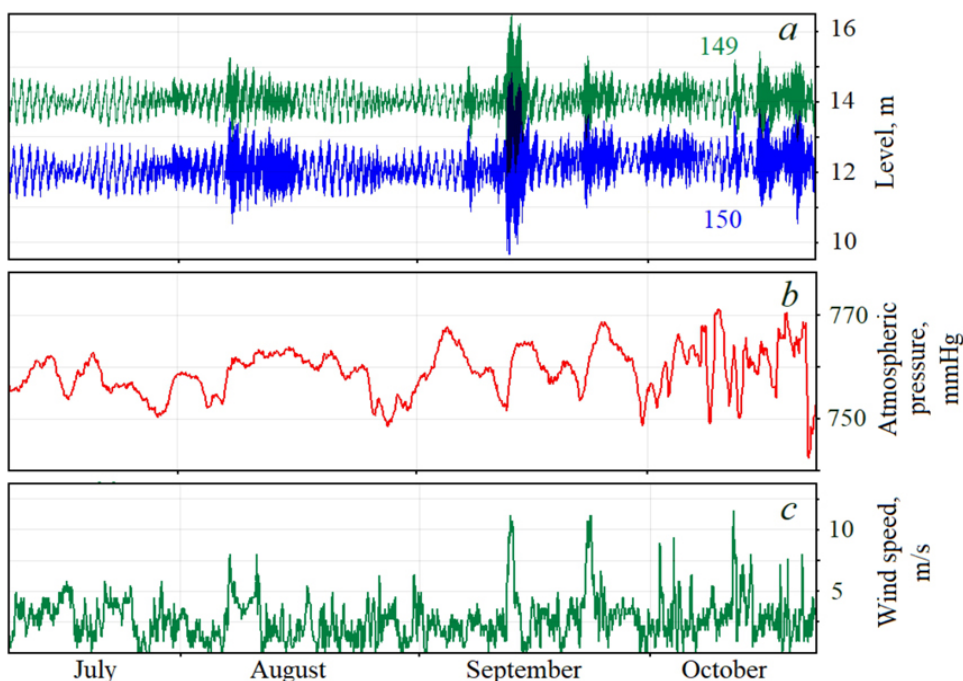


**Fig. 2.** Temporal variations in sea level fluctuations (a), recorded by devices 149 and 150; fluctuations in atmospheric pressure (b); and the wind velocity vector magnitude (c), recorded by the Vantage Pro2 Weather Station during the summer-autumn period of 2021.

allows for the identification of features within the analyzed time series. In this expression,  $G(\omega)$  is the gain coefficient, which is a dimensionless quantity, while the phase values  $\varphi(\omega)$  are expressed in radians between the time series of the device pair at each frequency.

The transfer function is a complex function of frequency  $k(j\omega) = K(\omega)e^{-j\varphi(\omega)}$ , known as the operator's transfer function. Its magnitude  $K(\omega)$  and argument  $\varphi(\omega)$  indicate how the amplitude and phase of each harmonic component of the spectrum of the transformed function change after the application of a linear operator [15]. In harmonic analysis, the magnitude of the transfer function  $K(\omega)$  is referred to as the amplitude-frequency characteristic, while the argument  $\varphi(\omega)$  is known as the phase-frequency characteristic of the operator.

### Waves propagating into open sea

The transfer function diagram in the direction from device 149 to device 150 (Fig. 3c) – toward the open sea – highlights energy peaks dur-

ing short wind wave periods of 2-3 seconds, as well as at a period of approximately 14.2 seconds, which corresponds to swell waves. Additionally, there are sea level fluctuations with periods of 3.6 minutes within the range of infragravity waves – 0.3 to 7 minutes [16] – and fluctuations extending somewhat beyond the range, with a period of 8.8 minutes. The work of Longuet-Higgins and Stewart [7] confirmed a hypothesis made in 1962 [17], which states that although the incident swell dissipates in the surf zone over shallow water, the forced infragravity waves of the second order (excited by nonlinear differential-frequency interactions of pairs of swell components) are released as free waves, reflecting off the shore and propagating seaward. In this context, the reduction in energy (due to shoaling) of the outgoing free radiated wave is approximately  $h^{-1/2}$ , and it is more gradual than the amplification of the incoming forced wave, which follows an  $h^{-5}$  relationship [7]. It is these leaky waves that correspond to the energy peaks of waves with periods of 3.6 and 8.8 minutes indicated in Fig. 3c.

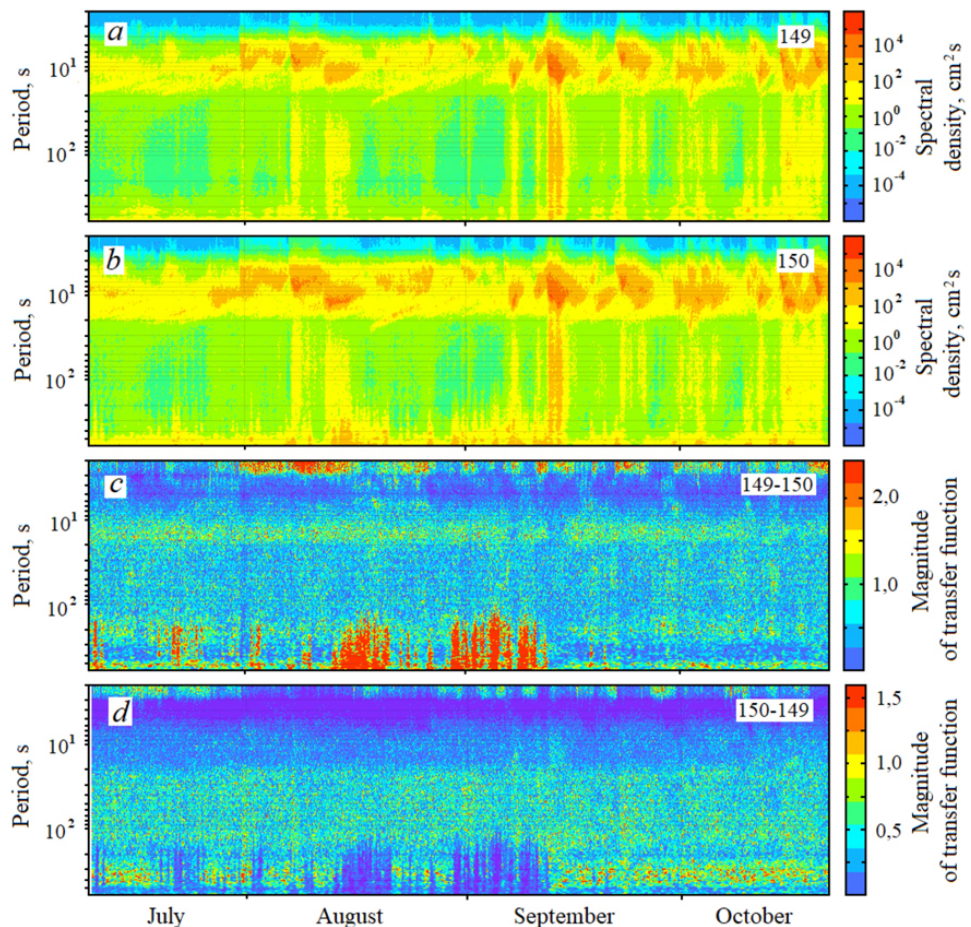


Fig. 3. Spectrograms of sea level fluctuations (a, b) and magnitude diagrams of the transfer function (c, d)

Another potential cause for the manifestation of waves with periods of 3.6 and 8.8 minutes may be Poincaré waves. Our depth measurements using an echo sounder-chart plotter in the observation area, along a line perpendicular to the line connecting the devices, showed that at distances from the shore of up to 10 km, the seabed profile is relatively flat and can be approximated by a model with a linear slope  $h(x) = \alpha x$ , where  $h$  is the depth,  $\alpha \approx 0.011$  is the slope of the seabed, and  $x$  is the coordinate in the direction away from the shore. The mathematical expression for describing Poincaré standing waves over a flat sloping bottom is given by the zeroth-order Bessel function [18]:

$$\zeta(\omega, x) = \zeta_{\text{shore}} J_0(a\sqrt{x}), \text{ где } a = 2\omega / \sqrt{g\alpha} \quad (1)$$

Here,  $g$  is the acceleration due to gravity,  $\omega = (2\pi)/(\text{period})$  is the angular frequency, and  $\zeta_{\text{shore}}$  is the amplitude at the shore.

Using equation 1, the normalized sea surface elevations were calculated as functions of the distance from the shore  $x$  for the standing wave periods of 3.6 and 8.8 minutes, as determined from the magnitude diagram of the transfer function shown in Fig. 3c. The calculation indicated the possibility of the existence of Poincaré standing waves with the observed periods. At a distance of approximately 450 m from the shore, where the instruments were installed, amplitudes close to the maximum were observed. Since these standing waves have a progressive nature along the shore [4] – along the line connecting the devices – the wave meters are expected to record progressive

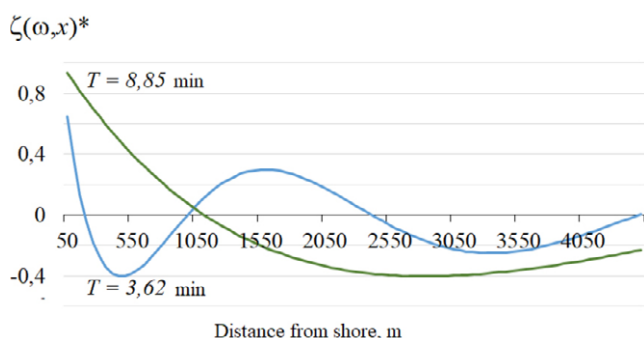


**Fig. 4.** The normalized standing wave amplitude  $\zeta(\omega, x)^*$ , with periods of 3.6 and 8.8 minutes, varies with distance from the shoreline.

waves with the specified periods and a direction of propagation parallel to the line connecting the devices, and as measurements indicate, seaward.

### Waves propagating along the coast

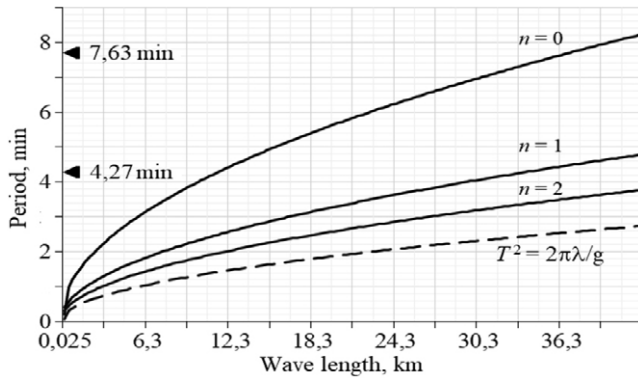
The transfer function magnitude diagram for waves propagating towards the shore (Fig. 3d) differs significantly from the previous one, which showed waves propagating away from the shore, except for the energy at periods of short wind waves of 2-3 seconds. A broad band of wave periods in the IG range from 20 to 110 seconds is prominent, and it is reasonable to assume that these waves are infragravity waves, considering their significant amplification during storms (Fig. 3a, b).

Figure 3d also shows a narrower band of waves with greater energy, with periods from 4.27 to 7.63 minutes. These can be attributed to edge waves, which are excited by energy from two sources. Firstly, these are IG waves propagating towards the shore, which, according to numerous studies, can transfer their energy to edge waves. Another source is the seaward-propagating free waves that can be reflected back towards the shore from a turning point on a sloping beach or shelf, generating edge waves. A portion of this energy is radiated outward into the ocean [7]. Models have also been developed for the resonant excitation of edge waves resulting from the nonlinear interaction of frequency differences between pairs of components of obliquely incident swell [19].

Let's consider the possibility of generating edge waves with the periods mentioned above for the specific bathymetry profile in the vicinity of Cape Svobodny. Since the bathymetric profile is relatively flat at a distance of about 10 km from the shore, the alongshore structure of edge waves can be described using the dispersion relation for Stokes waves in the approximation of a flat, sloping bottom [16]:

$$\omega_n^2 = gk \sin[(2n + 1)\beta], \quad (2)$$

where  $\omega_n$  is the frequency of the  $n$ th mode of the edge wave,  $g$  is the acceleration due to gravity,  $k$  is the alongshore wavenumber, and  $\beta$  is the bottom slope angle.



**Fig. 5.** Dispersion diagram of edge waves for three modes. Observed wave periods are marked with vertical lines. The Poincaré wave continuum lies below the  $T^2 = 2\pi\lambda/g$  curve, which represents the dispersion relation for shallow water waves.

The periods of generation of edge waves are limited by the value of  $T^2 = 2\pi\lambda/g$  ( $k \geq \omega^2/g$  [20]), and for any bottom slope angle  $\beta$ , there is always a limited number of edge wave modes  $n \leq \pi/4\beta - 1/2$  [16].

Using formula (2), the dispersion diagram for the first three modes of edge waves has been calculated, shown in Fig. 5. The vertical axis is marked with values corresponding to the observed wave periods within the range of IG wave periods. It can be seen that edge waves with a period of 7.63 minutes can be excited for the zero mode, and those with a period of 4.27 minutes can be excited for the first mode as well. Therefore, the calculation shows that edge waves with periods corresponding to the observed energy peaks are possible in the coastal zone of Cape Svobodny.

Using Eckart's [21] solution to the shallow water equations, the cross-shore profiles of edge waves with periods of 4.27 and 7.63 minutes were calculated for various modes as a function of distance from the shoreline. The expression for the velocity potential is:

$$\varphi(x) = e^{-kx} L_n(2kx), \quad (3)$$

where  $x$  is the distance from the shoreline,  $k$  is the wavenumber, and  $L_n$  is the Laguerre polynomial. Figure 6 shows the calculated mode profiles for edge waves with periods of 4.27 and 7.63 minutes. It can be seen that the cross-shore profiles for different periods have a similar character, but the modes with longer periods decay more slowly as they move away from the shore.

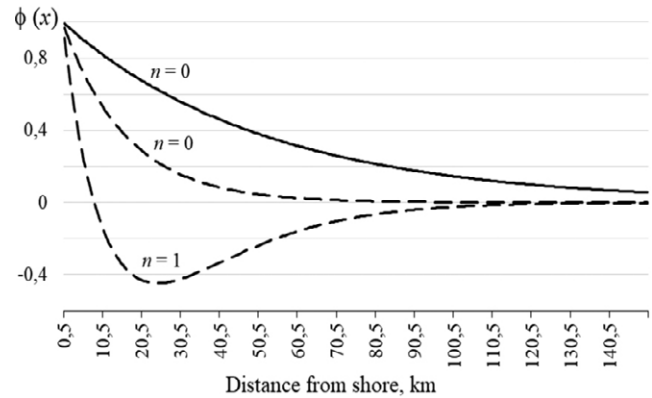


**Fig. 6.** Cross-shore profile shapes for edge wave modes with periods of 7.63 minutes (solid line) and 4.27 minutes (dashed line).

The analysis suggests the potential for generating edge waves with periods of 4.27 and 7.63 minutes. However, it does not definitively answer whether the observed waves are edge waves or another type. When investigating the structure of waves excited by energy transfer from IG waves, a challenge arises due to the similarity of edge wave and leaky wave modes at short distances from the shore on a flat beach. In [20], a criterion  $k \geq \omega^2/g$  is given, which separates the existence regions of edge waves with Poincaré and leaky waves. However, these waves may still exist with identical periods. Distinguishing them requires observations with two instruments along the length and direction of propagation, as demonstrated above.

### Influence of seawater temperature fluctuations on the propagation of waves with periods greater than 3 minutes

Another interesting factor affecting the propagation of waves with periods longer than 3 minutes is the influence of seawater temperature fluctuations. As seen in the transfer function magnitude diagrams (Fig. 7a, b), two significant events with anomalous transfer function magnitude values are observed in the period range of 3–100 minutes during August and September. The phase difference spectrograms (Fig. 7c, d) do not show substantial deviations for these events. These events are associated with significant temperature fluctuations, with periods shorter than diurnal (Fig. 7e), as opposed to longer periods spanning several days (Fig. 7f).

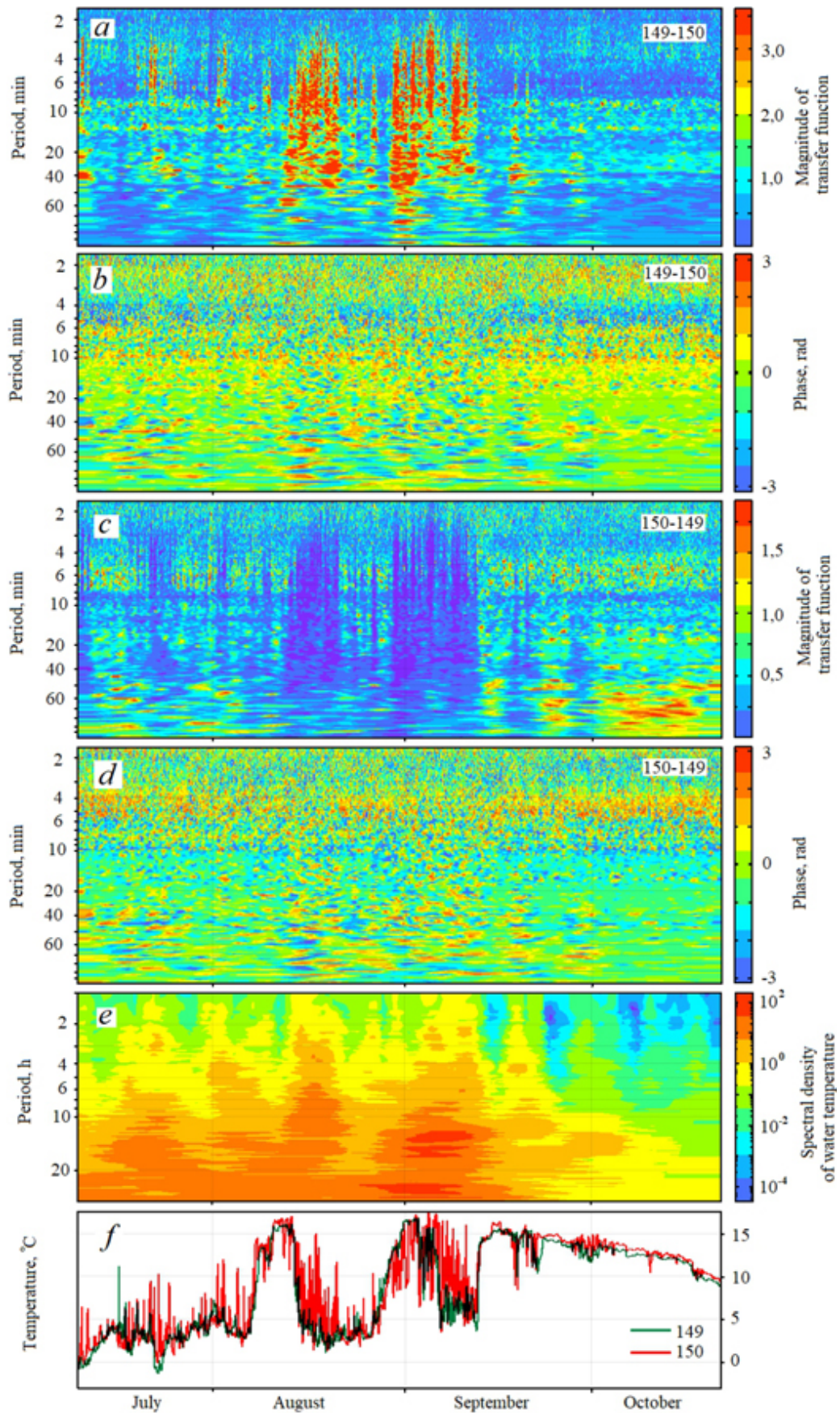


**Fig. 7.** Transfer function magnitude diagrams (a, b) and phase difference spectrograms (c, d) for sea level fluctuations (periods: 1–100 minutes), along with time series (f) and spectral density of seawater temperature fluctuations for instrument 150 (e).

Research in [22] shows that for seawater temperature fluctuations (1–80 hours), spectral peaks are identified for instrument 150 at periods of 25.5, 16.7, 12.9, and 6.7 hours, and for instrument 149 at periods of 13.2, 6.5, and 5.3 hours. However, the coherence for the temperature time series is significantly below the confidence level. The periods of the spectral peaks in seawater temperature fluctuations for periods longer than 5 hours do not coincide with the periods of the sea level fluctuation peaks. This indicates that these temperature fluctuation peaks are driven by internal waves. Furthermore, the temperature fluctuation spectrum for instrument 150 exhibits peaks at periods of 25.5 and 16.7 hours, which fall within the range of near-inertial internal waves.

It is evident that significant temperature fluctuations within the period range of 3–100 minutes,

corresponding to internal waves with amplitudes exceeding 7 °C, disrupt edge waves with periods of 4.27 and 7.63 minutes (Fig. 7c) propagating along the coast, as well as leaky waves with periods of 3.6 and 8.8 minutes propagating towards the sea (Fig. 7a). Energy transfer to internal waves with periods of 3–100 minutes (Fig. 7e) originates from longer internal waves with periods close to semi-diurnal and diurnal cycles. [22] proposes a mechanism of baroclinic instability to explain the energy transfer from larger to smaller scales.

### Wind waves in the vicinity of Cape Svobodny

The characteristics of wind waves and swell in this area are of interest, as it is actively used for fishing. Figure 8 shows the calculated spectral densities of wave activity in the range from 2

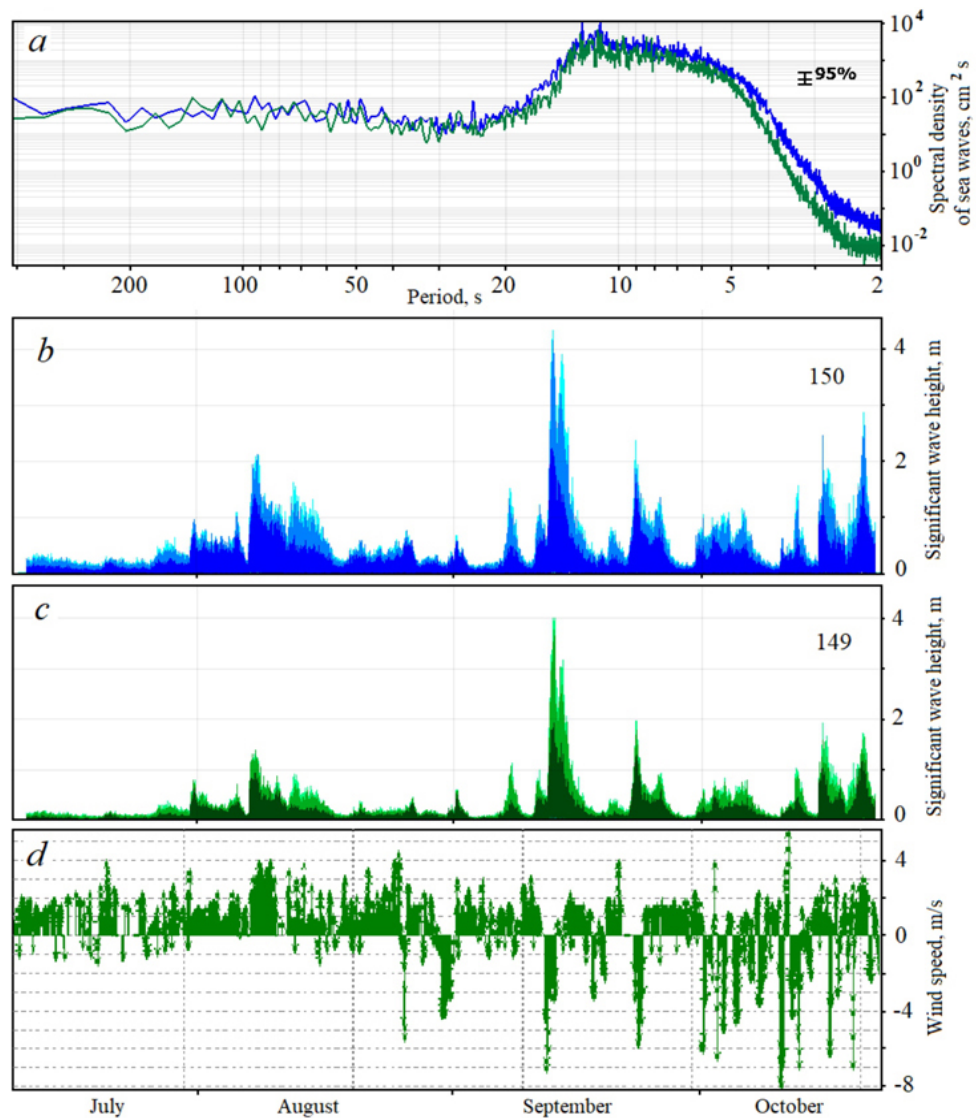


**Fig. 8.** Wave spectral densities (a); significant wave height for periods of 5, 8, and 11.5 seconds (b, c), highlighted in different shades (dark = 5 seconds); wind speed vectors recorded by the Vantage Pro2 Weather Station (d). The positive direction of the wind speed vectors corresponds to northerly winds.

to 200 seconds, encompassing both wind waves and swell. The curves in the 2–20 second range lack distinct peaks, including a defined wind wave band. Our current and previous research have shown that there is also no pronounced modal structure in the infragravity wave range.

In physical oceanography, the term significant wave height, denoted by  $H_s$ , is used to characterize waves. It is defined as the average wave height from trough to crest of the highest one-third of waves,  $H_{1/3}$ .

$$H_{1/3} = \frac{1}{\frac{1}{3}N} \sum_{m=1}^{\frac{1}{3}N} h_m, \quad (4)$$

The  $h_m$  values represent individual wave heights, sorted in descending order ( $m = 1$  to  $N$ ), considering only the highest one-third for alignment with visual observations. Significant wave height can also be defined as four times the standard deviation of the surface height or as four times the square root of the zero order moment [3].

Figure 8b, c shows graphs depicting the variation of significant wave height for periods of 5, 8, and 11.5 seconds, with the darker shade representing a period of 5 seconds. Wind waves and swell at instrument 150 are approximately 12 % higher than at instrument 149, which is slightly sheltered by the cape from waves originating from the Sea of Okhotsk. The highest wave heights were observed during sustained, approximately 24-hour long, southerly winds associated with a cyclone that passed over the observation area. A short-duration but strong wind with speeds up to 8 m/s does not contribute to the generation of wave heights comparable to those during a cyclone; in this case, they are half as high.

## Conclusion

This study analyzes various wave types in the waters off Cape Svobodny (southeastern coast of Sakhalin Island). Data were collected using two autonomous wave and seawater temperature recorders, ARV 14K, and a Vantage Pro2 Weather Station in 2021. Five-month time series of sea level and temperature fluctuations with a one-second sampling rate were employed. Atmospheric pressure and wind speed were recorded with an hourly sampling rate.

Spectral analysis revealed that wave spectral densities in the range of 2–600 seconds lack pronounced peaks. Wave energy at instrument 149 is lower than at instrument 150, which can be attributed to the sheltering effect of Cape Svobodny. An increase in energy within the infragravity wave band (periods of 20–250 seconds) is observed during storms, but without a distinct modal structure.

Waves with periods of 14.2 seconds, 3.6 minutes, and 8.8 minutes were investigated. The Longuet-Higgins and Stewart theory explains the short waves associated with swell scattering in the surf zone. Free waves are also generated in this process. The Lamb model and Bessel function confirmed the existence of leaky waves with periods of 3.6 and 8.8 minutes.

Wave processes propagating towards the shore include waves with periods from 20 to 110 seconds, as well as alongshore processes with periods of 4.27–7.63 minutes. Edge wave generation was explored for the bathymetric profile near Cape Svobodny using the dispersion relation for Stokes waves. Seawater temperature fluctuations impact the propagation of waves with periods longer than 3 minutes, disrupting both edge waves and leaky waves. Internal waves with periods of 3–100 minutes and amplitudes exceeding 7 °C affect the energy of short-period waves.

Analysis of wind wave and swell characteristics revealed the absence of significant wave activity in the period range of 2–20 seconds. The highest wave heights were observed during sustained southerly winds associated with a cyclone, while strong winds up to 8 m/s did not generate such high waves.

## References

1. Abuzyarov Z.K. 1981. [*Sea waves and its forecasting*]. Leningrad: Gidrometeoizdat, 166 p.
2. *Wind, waves and seaports*. Authors: Galenin B.G., Duginov B.A., Krivitskii S.V., Krylov Yu.M., Podmogil'nyi I.A. 1986. Leningrad: Gidrometeoizdat, 264 p.
3. Holthuijsen L.H. 2007. *Waves in oceanic and coastal waters*. Cambridge University Press, 387 p. <https://doi.org/10.1017/cbo9780511618536>
4. Efimov V.V., Kulikov E.A., Rabinovich A.B., Fain I.V. 1985. [*Waves in the boundary regions of the ocean*]. Leningrad: Hydrometeoizdat, 280 p.
5. Munk W.H., Snodgrass F.E., Wimbush M. 1970. Tides off-shore: Transition from California coastal to deep-

- sea waters. *Geophysical Fluid Dynamics*, 1(1-2): 161–235. <https://doi.org/10.1080/03091927009365772>
6. Mysak L.A. **1980**. Topographically trapped waves. *Annual Review of Fluid Mechanics*, 12: 45–76. <https://doi.org/10.1146/annurev.fl.12.010180.000401>
  7. Herbers T.H.C., Elgar S., Guza R.T. **1995**. Generation and propagation of infragravity waves. *Journal of Geophysical Research: Oceans*, 100(C12): 24863–24872. <https://doi.org/10.1029/95jc02680>
  8. Brunner K., Rivas D., Lwiza K.M.M. **2019**. Application of classical coastal trapped wave theory to high-scattering regions. *Journal of Physical Oceanography*, 49: 2201–2216. <https://doi.org/10.1175/jpo-d-18-0112.1>
  9. Plekhanov F.A., Kovalev D.P. **2016**. [A program for complex processing and analysis of time series of sea level data based on the author's algorithms]. *Geoinformatics*, 1: 44–53.
  10. Kovalev D.P. **2018**. *Кыма: The software*. RU 2018618773. No. 2018612587, application 20.03.2018; publ. 19.07.2018. (In Russ.).
  11. Otnes R., Enokson L. **1982**. [*Applied time series analysis*]. Moscow: Mir, 432 p.
  12. Yaffee R.A., McGee M. **2000**. *Introduction to time series analysis and forecasting with applications of SAS and SPSS*. New York: Academic press, 528 p.
  13. Bendat J.S., Piersol A.G. **2010**. *Random data: Analysis and measurement procedures*. New York: John Wiley & Sons, 640 p. <http://dx.doi.org/10.1002/9781118032428>
  14. Denman K.L. **1975**. Spectral analysis: a summary of the theory and techniques. *Fisheries and Marine Service, Report No. 539*. 37 p.
  15. Marple S.L. **1987**. *Digital spectral analysis: with applications*. New Jersey: Prentice Hall, 390 p.
  16. Rabinovich A.B. **1993**. [*Long gravitational waves in the ocean: capture, resonance, radiation*]. Leningrad: Gidrometeoizdat, 240 p.
  17. Longuet-Higgins M.S., Stewart R.W. **1962**. Radiation stress and mass transport in surface gravity waves with application to 'surf beats'. *Journal of Fluid Mechanics*, 13: 481–504. <https://doi.org/10.1017/s0022112062000877>
  18. Lamb H. **1945**. *Hydrodynamics*. 6th ed. New York: Dover publications. (Art. 260–261, p. 445–450). <https://doi.org/10.5962/bhl.title.18729>
  19. Foda M.A., Mei C.C. **1981**. Nonlinear excitation of long-trapped waves by a group of short swells. *Journal of Fluid Mechanics*, 111: 319–345. <https://doi.org/10.1017/s0022112081002401>
  20. Holman R.A., Bowen A.J. **1984**. Longshore structure of infragravity wave motions. *Journal of Geophysical Research: Oceans*, 89(C4): 6446–6452. <https://doi.org/10.1029/jc089ic04p06446>
  21. Eckart C. **1951**. *Surface waves on water of variable depth: Lecture Notes*. Marine Physical Laboratory, Scripps Institute Oceanography. Wave Report, 100(S10). 99 p.
  22. Kurkin A., Kovalev D., Kurkina O., Kovalev P. **2023**. Features of long waves in the area of Cape Svobodny (South-Eastern part of Sakhalin Island, Russia) during the passage of cyclones. *Russian Journal of Earth Sciences*, 23, ES3003. <https://doi.org/10.2205/2023es000852>

## About the Authors

Employees of the Laboratory of wave dynamics and coastal currents, Institute of Marine Geology and Geophysics of the Far Eastern Branch of RAS, Yuzhno-Sakhalinsk, Russia:

**Kovalev, Dmitry P.** (<https://orcid.org/0000-0002-5184-2350>), Doctor of Physics and Mathematics, Head of the laboratory, [d.kovalev@imgg.ru](mailto:d.kovalev@imgg.ru)

**Kovalev, Peter D.** (<https://orcid.org/0000-0002-7509-4107>), Doctor of Engineering, Leading Researcher, [p.kovalev@imgg.ru](mailto:p.kovalev@imgg.ru)

**Borisov, Aleksander S.** (<https://orcid.org/0000-0002-9026-4258>), Cand. Sci. (Engineering), Senior Researcher, [a.borisov@imgg.ru](mailto:a.borisov@imgg.ru)

**Kirillov, Konstantin V.** (<https://orcid.org/0000-0002-0822-3060>), Researcher, [k.kirillov@imgg.ru](mailto:k.kirillov@imgg.ru)

## Об авторах

Сотрудники лаборатории волновой динамики и прибрежных течений, Институт морской геологии и геофизики ДВО РАН, Южно-Сахалинск, Россия:

**Ковалев Дмитрий Петрович** (<https://orcid.org/0000-0002-5184-2350>), доктор физико-математических наук, руководитель лаборатории, [d.kovalev@imgg.ru](mailto:d.kovalev@imgg.ru)

**Ковалев Петр Дмитриевич** (<https://orcid.org/0000-0002-7509-4107>), доктор технических наук, ведущий научный сотрудник, [p.kovalev@imgg.ru](mailto:p.kovalev@imgg.ru)

**Борисов Александр Сергеевич** (<https://orcid.org/0000-0002-9026-4258>), кандидат технических наук, старший научный сотрудник, [a.borisov@imgg.ru](mailto:a.borisov@imgg.ru)

**Кириллов Константин Владиславович** (<https://orcid.org/0000-0002-0822-3060>), научный сотрудник, [k.kirillov@imgg.ru](mailto:k.kirillov@imgg.ru)

Received 20 June 2024  
Accepted 17 August 2024

Поступила 20.06.2024  
Принята к публикации 17.08.2024